Density-functional study of the Luttinger liquid behavior of the lithium molybdenum purple bronze $Li_{0.9}Mo_6O_{17}$

Z. S. Popović* and S. Satpathy
Department of Physics and Astronomy, University of Missouri, Columbia, Missouri 65211, USA
(Received 25 October 2005; revised manuscript received 1 June 2006; published 20 July 2006)

Using density-functional calculations, we study the electronic structure of the purple bronze $Li_{0.9}Mo_6O_{17}$, which has been proposed to be a paradigm system for the Luttinger liquid behavior. Our results show that the quasi-one-dimensional (1D) electron bands crossing the Fermi energy originate from the Mo atoms on the double zigzag chains with predominant Mo (d_{xy}) character and a Fermi surface that consists of two slightly warped planes, normal to the direction of the zigzag chains. The overall shape and dispersion of the bands as well as the calculated Fermi surface nesting vector are in excellent agreement with recent photoemission measurements. From constrained density-functional calculations of the Coulomb interactions and the calculated Fermi velocity, we estimate the values for the characteristic parameters of the Luttinger liquid, viz., the ratio of the spin-charge velocities to be $v_\rho/v_s \approx 1.8$ and the anomalous dimension characterizing the Fermi surface discontinuity to be $\alpha \approx 0.6$. The general agreement of these values with experiments further strengthens the case for the lithium molybdenum purple bronze as a Luttinger liquid.

DOI: 10.1103/PhysRevB.74.045117 PACS number(s): 71.20.−b, 71.10.Pm

I. INTRODUCTION

The Fermi liquid theory is successful in describing the behavior of the ordinary metals but breaks down in attempts to explain properties of one-dimensional (1D) systems. The Fermi liquid behavior is characterized by the Landau quasiparticles, which are low-energy single particle excitations, while, in sharp contrast to this, the low-energy excitations of the Luttinger liquid in 1D are collective excitations and exhibit the spin-charge separation. The existence of the collective excitations is based on a special property in 1D, viz., that all electron-hole excitations with a fixed momentum near the Fermi energy E_F cost the same energy. Two key features of the Luttinger liquid are the spin-charge separation, where the spin and the charge degrees of freedom are completely separated into collective density waves ("spinons" and "holons") that propagate with different velocities, and the power-law dependence of the correlation functions, which is characterized by the anomalous dimension.[1]

The idea of the Luttinger liquid goes back some 50 years or so. In a seminal paper, Tomonaga[2] showed that in 1D, the problem of interacting electrons is exactly solvable by bosonization. Quite remarkably, the problem of the interacting electrons in 1D reduces to the problem of noninteracting bosons, if one linearizes the band dispersion about the Fermi energy. Later, Luttinger[3] introduced the model with strictly linear dispersion, which was then solved exactly by Mattis and Lieb.[4] Subsequently, Haldane[5] argued that the generic features of interacting electrons in 1D are described by the low-energy physics of the Tomonaga-Luttinger model, much like the celebrated Fermi liquid theory in 3D.

A key feature needed for the experimental realization of the Luttinger liquid is a 1D band dispersion. While truly 1D systems such as the carbon nanotubes are currently being studied,[6] it is also recognized that 3D crystals with quasi-1D band structures might actually be the better systems to study, since it is easier to grow quality single crystals in a controlled fashion. Recently, the lithium molybdenum purple bronze has been identified as a possible paradigm system for studying the Luttinger liquid behavior.[7] Recent angle-resolved photoemission spectroscopy (ARPES) data[8,9] have indicated the presence of a 1D band crossing the Fermi surface and have provided evidence for the two main characteristics of the Luttinger liquid, the anomalous dimension and the spin-charge separation.

In this paper, we study the electronic band structure of the lithium molybdenum purple bronze $Li_{0.9}Mo_6O_{17}$ from density-functional calculations and connect our results with the predictions of the Luttinger liquid model.

II. CRYSTAL STRUCTURE

Molybdenum bronzes are a class of solid oxides exhibiting an intense color, with a chemical composition given by the formula $A_xM_yO_z$, where A stands for an alkali metal or Tl and M stands for a variety of metal atoms such as Mo or W.[10] The lithium molybdenum purple bronze $Li_{0.9}Mo_6O_{17}$, the subject of our paper, is a quasi-1D metal at room temperature with a highly anisotropic conductivity along the principal crystal axes. It is metallic at room temperature and, as temperature is reduced, undergoes a phase transition at 24 K, finally becoming a superconductor below 1.9 K.[10,11] There is a small hump in the specific heat[11] and a resistivity upturn[12,13] at the transition point at 24 K, however no noticeable change in the lattice through the metal-insulator transition is observed.[14]

Unlike the blue bronze[9] or the other purple bronzes $A_{0.9}Mo_6O_{17}$ [A=K, Na (Ref. 15), Tl (Ref. 16)], which are 2D metals exhibiting charge density waves (CDW), there is no evidence for the CDW either in the magnetic susceptibility[17] or in the optical experiments.[14,18] There is also no indication of any Peierls instability in the x-ray diffraction,[9] where no structural distortion has been observed, strengthening further the viewpoint that the transition at 24 K is not a CDW transition. The absence of a CDW is an important feature of the $Li_{0.9}Mo_6O_{17}$, leading to a unique quasi-1D metal, where any

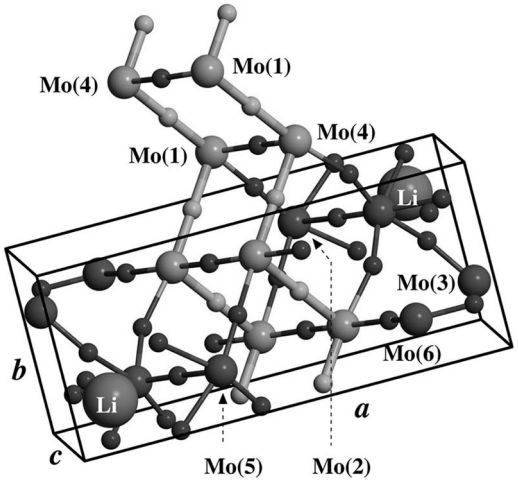

FIG. 1. The unit cell of $Li_{0.9}Mo_6O_{17}$, indicating the 1D zigzag chains that run along the b direction and are responsible for the quasi-1D bands crossing the Fermi energy.

Luttinger liquid behavior is not complicated by the existence of a CDW instability lingering nearby.

The crystal structure of $Li_{0.9}Mo_6O_{17}$ is monoclinic, with the space group $P2_1/m$ (No. 11 in the International Tables). The unit cell parameters are $a=12.762$ Å, $b=5.523$ Å, $c=9.499$ Å, and $\beta=90.61°$ with the atomic positions given by Onoda *et al.*[19] The unit cell contains six crystallographically different Mo sites (Fig. 1), with two molybdenum atoms, Mo(3) and Mo(6), in a tetrahedral MoO_4 surrounding, while the remaining four—including the Mo(1) and Mo(4) on the zigzag chain—are in an octahedral surrounding, forming the MoO_6 octahedra. The zigzag chains run along the b direction, forming a chain pair in the unit cell, which are well separated from chains in the neighboring cells as indicated in Fig. 2. The chains within the pair are laterally connected by the rungs of Mo(1)-O-Mo(4) atoms.

III. BAND STRUCTURE

The band structure calculations were performed within the local-spin-density approximation to the density-functional theory (DFT) using the linear muffin-tin orbitals method in

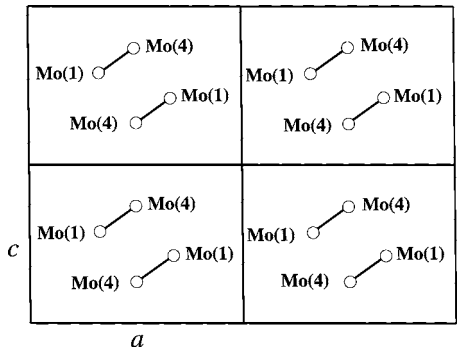

FIG. 2. Projection of the zigzag chains onto the ac plane. Pairs of chains belonging to different unit cells (four shown here) are well separated from one another. As a result, the largest band dispersions of the zigzag chain quasi-1D bands are along the b direction, normal to the plane of paper, along which the chains run.

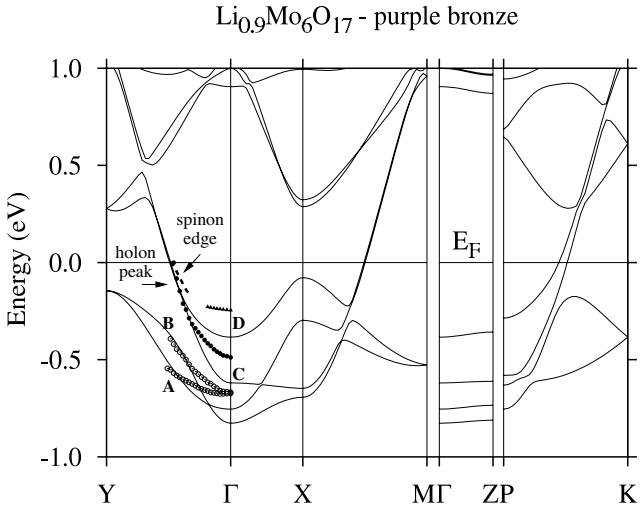

FIG. 3. Density-functional band structure of $Li_{0.9}Mo_6O_{17}$ close to the Fermi energy E_F (solid lines) compared to the ARPES data (points) along the Γ-Y direction. The data point sets marked A through D correspond to the peaks in the ARPES data, which are taken from Fig. 9(b) of Ref. 9. The labels "spinon edge" and the "holon peak" refer to the spin-charge excitations inferred from the ARPES in the linear band structure regime close to the E_F. The "spinon edge" cannot be clearly demarcated from the ARPES and in the figure it is only meant to be a guide. The collective excitations change over to the one-particle excitations as one goes deeper below E_F into the nonlinear regime of the band structure, show up as robust C and D peaks in the ARPES. The $\vec{k}$ points in the Brillouin zone are $Y=(0,0.5,0)$, $\Gamma=(0,0,0)$, $X=(0.003,0,0.291)$, $M=(0.003,0.5,0.291)$, and $Z=(0.216,0.0,0.0)$ in units of $2\pi/b$. The points P and K are indicated in Fig. 6.

the atomic spheres approximation[20] (LMTO-ASA) to solve the Kohn-Sham equations. There are 48 atoms in the unit cell [two formula units $(Li_{0.9}Mo_6O_{17})_2$], but since the crystal structure is loosely packed, it was necessary to insert a large number of empty spheres for accurate calculations, resulting in a total of 108 atomic spheres per unit cell. We used the von Barth–Hedin exchange-correlation potential[21] together with the generalized-gradient approximation of Perdew and co-workers.[22] The basis sets used are Mo($5s,5p,4d$), O($2s,2p,3d$), and Li($2s,2p,3d$), and 30 mesh points in the irreducible zone were used for the Brillouin zone integration. The band calculations were performed for the ideal crystal structure $LiMo_6O_{17}$ with no Li vacancy, and since lithium basically donates one electron, the Fermi energy E_F was determined by rigidly shifting it down by about 0.03 eV (0.1 less electron per formula unit) to take into account the 10% Li vacancy of the actual crystal structure. The same was done in the calculation of the Fermi surface as well.

The calculated band structure around the Fermi energy is shown in Fig. 3. The four bands forming the topmost valence region are separated from the $O(2p)$ bands, which are immediately below in energy, as seen from the projected density of states (DOS) (Fig. 4). The overall features of our band structure are in general agreement with the earlier, pioneering work of Whangbo and Canadell,[23] which studied the band structure of the molybdenum bronze with an empirical tight-

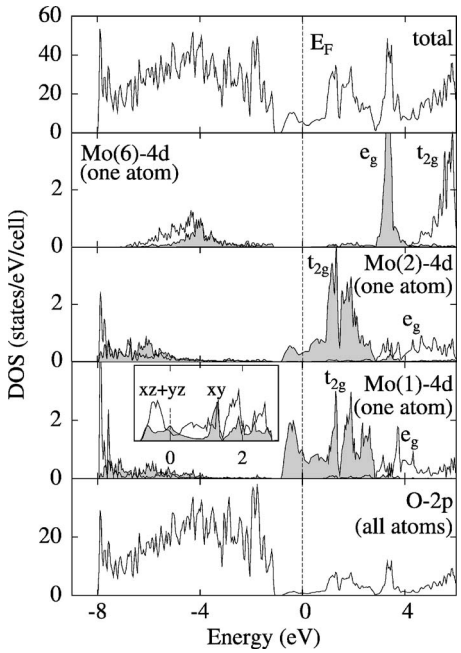

FIG. 4. Total and atom-and-orbital projected densities of states for $Li_{0.9}Mo_6O_{17}$. The bands near E_F originate from primarily the chain site Mo atoms [viz., Mo(1) and Mo(4), whose DOS's are very similar]. Mo(2) and Mo(6) are representative out-of-chain atoms. Mo(2), which is denoted by Mo′ in Fig. 5, contributes a significant amount to the bands near E_F owing to its proximity to the chains, while the contribution of the remaining out-of-chain Mo atoms is minimal. The inset in the Mo(1) panel shows the contributions of the xy vs the $xz+yz$ orbitals of Mo(1) in a local coordinate system, with the x and y axes pointing along the Mo-O-Mo bonds and the z axis, along the rung connecting the two chains. The inset indicates the quasi-1D bands crossing E_F to originate mostly from the chain site Mo(d_{xy}) orbitals (see also Fig. 5), with a significant admixture from the $xz+yz$ orbitals.

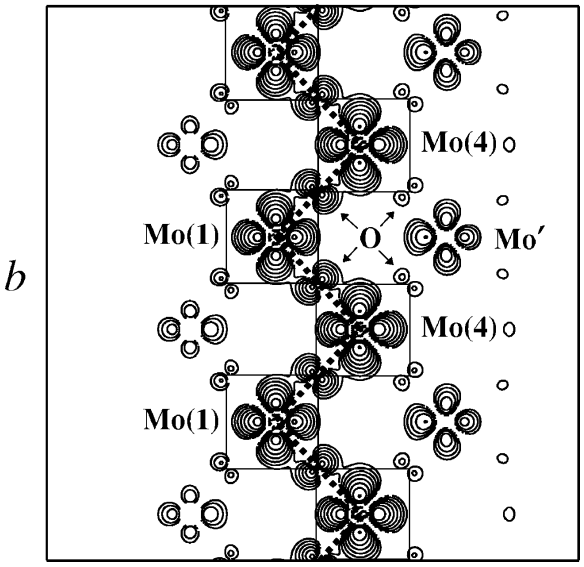

FIG. 5. Charge-density contour plot of the quasi-1D bands near E_F on a plane containing the zigzag chain. The second chain in the unit cell is stacked on top of the chain shown, directly above the plane of the paper and connected to it by the Mo-O-Mo rungs at every Mo atom. Energy window for the charge-density plot is E_F and 0.1 eV below it. Contour values are $\rho_n=2.7\times10^{-3}\times10^{0.21n}e^-/$ Å^3, with $n=0,1,2,\ldots,7$.

binding method. However, the overall widths of the tight-binding bands were too small by a factor of about two to three as compared to the density-functional bands or the photoemission data.

The two bands crossing the Fermi energy exhibit a quasi-1D character: Their most prominent dispersion is for $\vec{k}$ varying along the length of the zigzag chain (Γ-Y or X-M line), while the dispersion along directions perpendicular to the chain, Γ-X or Γ-Z, is much smaller. The overall band width of the density-functional bands is in reasonable agreement with the photoemission data. The point where the quasi-1D bands cross E_F as measured from the Γ point, is calculated to be $k^F_{\Gamma Y}=0.487\pi/b$, in excellent agreement with the ARPES results[9] of $\approx 0.51\pi/b$.

The basic band structure near E_F, which originates from the chain site Mo(d) orbitals, is conveniently described in a local coordinate system with origin on the chain site Mo atoms and with the x and the y axes pointed approximately along the Mo-O-Mo bonds. In this coordinate system, the two quasi-1D bands crossing the Fermi energy originate from the Mo(d_{xy}) orbitals, while the lower two occupied bands of the four-band manifold (see the Γ-Y direction in Fig. 3) originate from the Mo($d_{yz}+d_{xz}$) orbitals. The orbital character of these quasi-1D bands is illustrated by the charge-density contour plot of Fig. 5, which clearly shows the Mo(d_{xy}) character of the bands.

The double chains serve a very important role in producing the quasi-1D bands by removing the xz/yz bands away from the Fermi energy. Below we will argue that it is the interchain interaction that is responsible for this. The four lowest bands at the Y point in the band structure of Fig. 3 have the chain site xz/yz character and because of the noncrossing rule, the upper two merge with the quasi-1D bands as seen from the band structure along the Γ-Y line.

Not counting the spin, there are all in all eight xz and yz orbitals per unit cell arising out of the chain site Mo atoms (two chains per cell, two Mo atoms on each chain, and two orbitals per atom), which split into four bonding and four antibonding states due to interaction within the chain between neighboring Mo atoms. The four bonding states which have the lower energy then split into two groups (again, bonding and antibonding) due to coupling between the chains, which are displaced along z with respect to each other. These latter two bonding states are the lowest in energy (two lowest bands along Γ-Y in Fig. 3), with a clear gap at the Y point, which separates them from the two antibonding states. For the quasi-1D bands originating from the Mo(d_{xy}) orbitals, while the *intra*chain bonding interaction is present ($V_{dd\pi}$),[24] the *inter*chain coupling is extremely weak ($V_{dd\delta}$), leading to the two nearly degenerate bands crossing the Fermi energy. Within this picture, by splitting the xz/yz bands by the interchain interaction and removing them away from E_F, the double chain serves an essential role in producing two clean xy bands crossing the Fermi energy. However, the price we had to pay for having the double chain structure

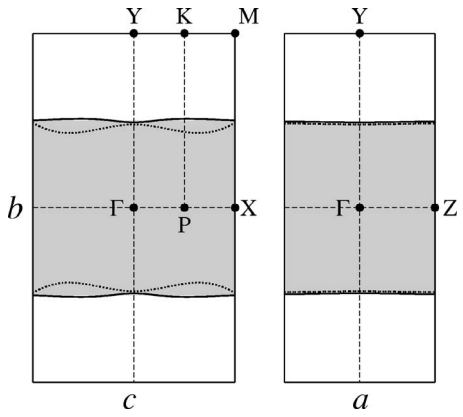

FIG. 6. Calculated Fermi surface for $Li_{0.9}Mo_6O_{17}$, indicating the two pairs of warped Fermi sheets. The shaded region is occupied.

is the presence of the two quasi-1D bands (one per chain) instead of just one, which would have produced a textbook example of a single 1D band crossing the Fermi energy.

The nominal chemical valence of the compound may be obtained with the following argument. Since two xz/yz bands derived from the chain site Mo atom are occupied in the unit cell, which has four such atoms, and each band can hold two electrons taking into account the spin, we have one electron occupied per chain site Mo atom in these bands. In addition, the two xy-like bands crossing the Fermi energy are half full, leading to the occupancy of two xy electrons in the unit cell including the spin or, equivalently, half an electron per Mo atom. This results in the nominal valence of Mo($d^{1.5}$) for the chain site atoms, while the out-of-chain Mo′ atoms have the valence Mo′(d^0), leading to the nominal valence of $Li^{+1}(Mo^{+4.5})_2(Mo'^{+6})_4O_{17}^{-2}$, where Mo (Mo′) refers to the chain site (out-of-chain) atoms. For the real crystal with 10% Li vacancy, electrons have to be depleted from the chain site Mo atom in the above formula.

The Fermi surface shown in Fig. 6 consists of two double sheets, the two quasi-1D bands producing one double sheet each. The sheets form slightly warped ac planes, perpendicular to the chain direction b. The warping, caused by the weak interchain interaction, is mainly along c with very little warping along the a direction, since the band dispersion along a is small. The calculated nesting vector $q=2\pi/b(0,0.487,0)$ is in agreement with the ARPES result[9] of $q\approx 2\pi/b(0,0.50,0)$. The topology of the Fermi surface is consistent with the highly anisotropic character of the measured conductivity, with ratios of about 250:10:1 for conductivities along the b, c, and a axes, respectively.[12,13]

IV. BAND STRUCTURE AND ARPES LINE SHAPES

Photoemission line shapes for $Li_{0.9}Mo_6O_{17}$ have been analyzed by Allen and coworkers[9] by using predictions[25,26] of the Tomonaga-Luttinger model for T=0 and a refined analysis using nonzero T by the same group is given is Refs. [7,27]. The key results of the theory are as follows. For the angle-integrated spectrum, the spectrum vanishes as power law $|E-E_F|^\alpha$ at the Fermi surface. For the angle-resolved spectrum and for momentum k inside the Fermi surface, the charge and spin excitations, the holons and spinons, show up as two peaks (the spinon as an edge if $\alpha>0.5$), while for momentum outside the Fermi surface, one gets an edge. This result is valid for a single band with linear dispersion at the Fermi energy.

In the purple bronze, we have two linear bands crossing the Fermi energy originating from the two zigzag chains. Since their electronic structures are weakly coupled, one would expect a holon-spinon pair for each of the two linear bands crossing E_F, which, however, cannot be resolved in the photoemission. As one moves deeper below E_F, the band dispersions are no longer linear, so that the excitations should become one-particle-like as opposed to the collective charge and spin excitations for the linear bands. If the electron correlation effects can be neglected, we may then compare the energy of the one-particle excitations observed from the ARPES much below E_F with the band structure theory. Thus for energies well below the Fermi surface, the holon peaks and the spinon edges in the ARPES will then go over to single-particle excitation peaks, which appear as robust C and D peaks in the ARPES.

In Fig. 3, we have indicated the ARPES data taken from Fig. 9(b) of Ref. 9 along the Γ-Y direction in the Brillouin zone. The spin-charge excitations marked by "spinon edge" and "holon peak" close to the E_F in the linear regime of the band structure are inferred from the ARPES data. Because the "spinon edge" can not be clearly determined from the ARPES since it is an edge rather than a peak, and more fundamentally because the momentum and the energy of the measured photoexcited electron is built up of the various spin-charge excitations, the spin and charge velocities are not extracted directly from the dispersion curves. Rather, they are determined by fitting the predicted Luttinger liquid lineshapes with the angle-integrated photoemission data.

The overall ARPES bandwidth is somewhat smaller than the width of the density-functional bands. In the Tomonaga-Luttinger model, the charge velocity is higher than the spin velocity and the ARPES data indicates this as shown in Fig. 3. If the electron interaction is spin independent, then the spin velocity equals the Fermi velocity v_F, while for the case of a spin-dependent interaction, the spin velocity is no longer the same as the Fermi velocity, but may be somewhat lower than v_F (e.g., in the one-band Hubbard model).[30] Since the spinon shows up as an edge in the ARPES, its position, as already mentioned, cannot be accurately determined to distinguish between the predictions of the spin-dependent vs the spin-independent interactions by comparing the spin velocity with the Fermi velocity calculated from the band structure. However, the spin velocity does seem to be a bit lower than the band structure v_F, while the charge velocity appears to be somewhat higher than the v_F.

Thus there are two distinguishing features in the ARPES that support the Luttinger liquid picture over the Fermi liquid picture. The first is the presence of two different excitations (holons and spinons) that disperse with two different velocities, the charge velocity v_ρ and the spin velocity v_s. There would be a single dispersion in the Fermi liquid theory. The second feature is the presence of the spinon edge, rather than a peak.

V. LUTTINGER LIQUID PARAMETERS

We now turn to the estimation of the two main characteristic parameters of the Luttinger liquid, viz., the anomalous dimension α and the velocities for the collective spin and charge excitations, v_s and v_ρ, respectively. We determine these parameters from the density-functional theory from a direct evaluation of the Coulomb interaction and the calculated Fermi velocity.

The Fermi velocity v_F for the noninteracting electrons can be computed by taking the derivative of the energy along the ΓY line: $\hbar v_F = \partial E(k_y)/\partial k_y|_{E_F} = 3.72$ eVÅ. For spin-independent interaction, this also equals the spin velocity v_s, while the charge velocity is enhanced by the factor $\beta = [1 + V(0)/(\pi\hbar v_F)]^{1/2}$. Here, $V(0)$ is the integral of the interaction $V(x)$ over all space in the continuum model and, for a 1D tight-binding model of interacting orbitals, we may estimate it from the expression: $V(0) = a(U_0 + \nu U_1 + \nu U_2 + \cdots)$, where U_0 (U_i) is the on-site (near-neighbor) Coulomb repulsion, a is the Mo-Mo distance ($a = 3.72$ Å), and $\nu = 2$ is the number of the various near neighbors.

Using an established procedure[28,29] within the framework of the "constrained" DFT, we have evaluated the Coulomb parameters for the chain-site Mo atom. We followed the approach used by Gunnarsson *et al.*,[28] setting to zero the hopping integrals for the d electrons of a single chain-site Mo(1) atom. The d occupancies for the other Mo atoms were fixed at integral values (d^3 in the present case), also by removing the hoppings. The U value may depend on how one constrains the other Mo $3d$ shells, but this dependency should be small for well-localized d orbitals.

Fully self-consistent calculations for two different configurations were performed and using the Slater's transition rules,[31] one obtains $U_0 = C_{3d}^{\mathrm{Mo}(1)}(n=4) - C_{3d}^{\mathrm{Mo}(1)}(n=3)$, where $C_{3d}^{\mathrm{Mo}(1)}(n)$ is the band center calculated with the fixed occupancy n of the Mo(1) atom. The on-site Coulomb repulsion estimated with this procedure is $U_0 = 6.4$ eV. The nearest-neighbor Coulomb repulsion U_1 may be estimated as $U_1 \sim e^2/\kappa a \approx 0.2$ eV, with $\kappa \approx 10$, which is consistent with the fact that the nearest-neighbor interaction U_1 in solids is typically a few tenths of an eV. Neglecting the further-neighbor Coulomb repulsions, we get $V(0) = 25.3$ eVÅ, which leads to the ratio for the spin-charge velocities to be $\beta = v_\rho/v_s = 1.8$, which is of the order of the experimental value[7] of $\beta \approx 2$. We hasten to add that even though this is the best value of the parameter one can get from the band theory at present, we consider it to be no better than a "good" estimate. It is nevertheless satisfying that our calculated Luttinger liquid parameters are close to those extracted from the experiments.

The anomalous dimension using the lowest-order perturbation theory[32] may be calculated as $\alpha^{(2)} = [V(0)/(2\pi\hbar v_F)]^2/2 = 0.59$. Experimental estimates from photoemission vary in the older literature between $\alpha = 0.6$–0.9,[7,9,33] depending on the theory used to fit the photoemission lineshapes. Refined estimates using Orgad's theory[34] of the finite-temperature lineshapes have just appeared in the literature,[27] which indicate the value of α to be temperature-dependent, varying between $\alpha = 0.9$ at $T = 300$ K to the value of 0.6 at lower temperatures between $T = 50$–200 K.

From a completely different type of experiment, Hager *et al.* have inferred the value of $\alpha = 0.62 \pm 0.17$ from the power-law behavior of the differential tunneling current using scanning tunneling spectroscopy for $T = 5$–55 K.[35] Thus there now seems to be a general concensus for the value of the anomalous dimension to be $\alpha \approx 0.6$ at $T = 0$ between the various experiments and theory. While the anomalous dimension could become renormalized in the Luttinger liquid theory due to the presence of the two bands at E_F and also due to the presence of the back scattering term, the general agreement between theory and experiment is nevertheless quite satisfactory, strengthening the case for $Li_{0.9}Mo_6O_{17}$ to be a paradigm Luttinger liquid.

We thank Jim Allen for many stimulating discussions and acknowledge support of this work by the U.S. Department of Energy (Grant No. DE-FG02-00ER45818) and the Petroleum Research Fund of the American Physical Society (Grant No. 40872-AC10).

*Permanent address: INN-"Vinča," P.O. Box 522, 11001 Belgrade, Serbia and Montenegro.

[1] For a review, see J. Voit, Rep. Prog. Phys. **58**, 977 (1995).
[2] S. Tomonaga, Prog. Theor. Phys. **5**, 544 (1950).
[3] J. M. Luttinger, J. Math. Phys. **4**, 1154 (1963).
[4] D. C. Mattis and E. H. Lieb, J. Math. Phys. **6**, 304 (1965).
[5] F. D. M. Haldane, J. Phys. C **14**, 2585 (1981).
[6] See, for example, M. Bockrath *et al.*, Nature (London) **397**, 598 (1999).
[7] G.-H. Gweon, J. W. Allen, and J. D. Denlinger, Phys. Rev. B **68**, 195117 (2003).
[8] J. D. Denlinger, G.-H. Gweon, J. W. Allen, C. G. Olson, J. Marcus, C. Schlenker, and L. S. Hsu, Phys. Rev. Lett. **82**, 2540 (1999).
[9] G.-H. Gweon, J. D. Denlinger, J. W. Allen, R. Claessen, C. G. Olson, H. Höchst, J. Marcus, C. Schlenker, and F. L. Schneemeyer, J. Electron Spectrosc. Relat. Phenom. **117-118**, 481 (2001).
[10] M. Greenblatt, Chem. Rev. (Washington, D.C.) **88**, 31 (1988).
[11] C. Schlenker, H. Schwenk, C. Escribefilippini, and J. Marcus, Physica B & C **135**, 511 (1985).
[12] M. Greenblatt, W. H. Carroll, R. Neifeld, M. Croft, and J. V. Waszczak, Solid State Commun. **51**, 671 (1984).
[13] M. Sato, Y. Matsuda, and H. Fukuyama, J. Phys. C **20**, L137 (1987).
[14] J. Choi, J. L. Musfeldt, J. He, R. Jin, J. R. Thompson, D. Mandrus, X. N. Lin, V. A. Bondarenko, and J. W. Brill, Phys. Rev. B **69**, 085120 (2004).
[15] G.-H. Gweon *et al.*, J. Phys.: Condens. Matter **8**, 9923 (1996); G.-H. Gweon J. W. Allen, J. A. Clack, Y. X. Zhang, D. M.

Poirier, P. J. Benning, C. G. Olson, J. Marcus, and C. Schlenker, Phys. Rev. B **55**, R13353 (1997).
[16] M. Ganne *et al.*, Solid State Commun. **59**, 137 (1986); K. V. Ramanujachary, T. B. Collins, and M. Greenblatt, Solid State Commun. **59**, 647 (1986).
[17] Y. Matsuda, M. Sato, M. Onoda, and K. Nakao, J. Phys. C **19**, 6039 (1986).
[18] L. Degiorgi, P. Wachter, M. Greenblatt, W. H. McCaroll, K. V. Ramanujachary, J. Marcus, and C. Schlenker, Phys. Rev. B **38**, 5821 (1988).
[19] M. Onoda, K. Toriumi, Y. Matsuda, and M. Sato, J. Solid State Chem. **66**, 163 (1987).
[20] O. K. Andersen, Phys. Rev. B **12**, 3060 (1975); H. L. Skriver, *The LMTO Method* (Springer, New York, 1983); O. Gunnarsson, O. Jepsen, and O. K. Andersen, Phys. Rev. B **27**, 7144 (1983).
[21] U. von Barth and L. Hedin, J. Phys. C **5**, 1629 (1972).
[22] J. P. Perdew and Y. Wang, Phys. Rev. B **45**, 13244 (1992); J. P. Perdew, K. Burke, and M. Ernzerhof, Phys. Rev. Lett. **77**, 3865 (1996).
[23] M. H. Whangbo and E. Canadell, J. Am. Chem. Soc. **110**, 358 (1988).
[24] W. A. Harrison, *Electronic Structure and the Properties of Solids* (Freeman, San Francisco, 1980).
[25] V. Meden and K. Schönhammer, Phys. Rev. B **46**, 15753 (1992).
[26] J. Voit, Phys. Rev. B **47**, 6740 (1993).
[27] F. Wang, J. V. Alvarez, S.-K. Mo, J. W. Allen, G.-H. Gweon, J. He, R. Jin, D. Mandrus, and H. Höchst, Phys. Rev. Lett. **96**, 196403 (2006).
[28] O. Gunnarsson, O. K. Andersen, O. Jepsen, and J. Zaanen, Phys. Rev. B **39**, 1708 (1989).
[29] Z. Zhang and S. Satpathy, Phys. Rev. B **44**, 13319 (1991).
[30] N. Nagaosa, *Quantum Field Theory in Strongly Correlated Electronic Systems* (Springer, Berlin, 1999).
[31] J. C. Slater, *Quantum Theory of Molecules and Solids* (McGraw-Hill, New York, 1974).
[32] See, for example, K. Schönhammer, cond-mat/9710330 (unpublished); *Interacting Electrons in Low Dimensions* (Kluwer Academic, Dordrecht, in press); cond-mat/0305035 (unpublished).
[33] G.-H. Gweon, Ph.D. thesis, University of Michigan (1999).
[34] J. W. Allen, Philos. Mag. B **81**, 377 (2001).
[35] J. Hager, R. Matzdorf, J. He, R. Jin, D. Mandrus, M. A. Cazalilla, and E. W. Plummer, Phys. Rev. Lett. **95**, 186402 (2005).